GLOBAL MAPPING OF ASTEROID 1 CERES WITH HST/ACS. Jian-Yang Li[1], Lucy A. McFadden[1], Joel Wm. Parker[2], Eliot F. Young[2], and Peter C. Thomas[2], [1]Department of Astronomy, University of Maryland, College Park, MD 20742 (jyli@astro.umd.edu), [2]Department of Space Studies, Southwest Research Institute, Boulder, CO 80302, [3]Center for Radiophysics and Space Research, Cornell University, Ithaca, NY 14853.

Introduction: Asteroid 1 Ceres is one of the two targets of NASA's Discovery Program mission scheduled to launch in June 2007. To support the mission, HST/ACS (advance camera for surveys) images of Ceres were obtained in 2003/04 through three filters centered at 535 nm, 335 nm and 223 nm. Ceres was 2.61 AU from the Sun and 1.65 AU from the Earth during the observation, and was resolved to ~750 pixels in the images with ~30 km/pixel, or 3.5° longitude/latitude projected at the sub-Earth point on Ceres. These images almost evenly cover the rotation of Ceres. The shape model and the rotational period have been accurately determined [1]. The photometric properties of the surface of Ceres have been studied, and the first surface maps at above three wavelengths have been constructed from these images (Li *et al.*, 2006). In this abstract we will discuss the techniques used to generate the maps of Ceres from HST/ACS images.

Data Reduction: Six consecutive HST orbits were used to obtain images covering one full rotation of Ceres of 9.075 hours. Images were reduced through the standard HST/ACS data reduction pipeline, then manually corrected for geometric distortion and rotated to celestial north up. The rotation of Ceres can be easily recognized from the movement of surface features such as a bright spot in the imaging sequence (Fig. 1). According to the shape model developed [1], the sub-Earth and sub-solar latitude during the observation are +2.1° and +3.9°, respectively. Thus most of the surface can be mapped well except for the two poles.

Photometric Modeling: In order to combine all images and construct global maps, photometric correction has to be applied. Since all these images were obtained in one rotation, there is no correction for phase function needed, and only limb darkening needs to be corrected. We tried three different models to fit the limb profile of Ceres, including Hapke model for a rough surface, Minnaert model, and a modified Minnaert model, to ensure good mathematical modeling for the limb darkening.

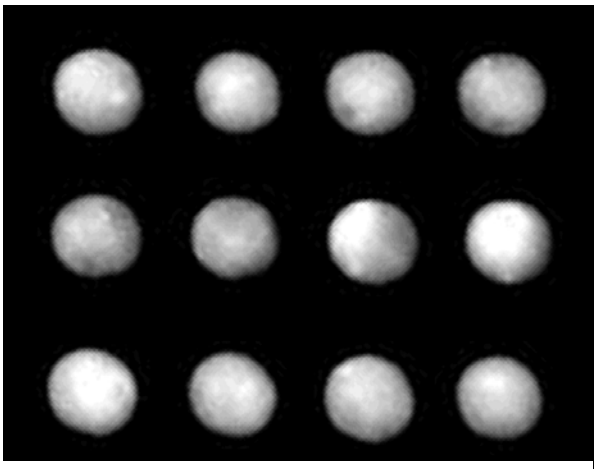

Fig. 1. HST/ACS image sequence of Ceres' rotation. Sequence runs from left to right then from top to bottom.

Hapke model fits resulted in good fit for the center part of the disk with the incidence angle (i) and emission angle (e) <50° with a high roughness parameter of 50°. The model scatter is less than 2%, and for the outskirt of the disk, the model scatter grows rapidly to higher than 14%. Minnaert model describes the limb profile as $r \propto \cos^{k}(i) \times \cos^{(k-1)}(e)$, where Minnaert parameter k describes how fast the limb darkens. For the surface of Ceres, the Minnaert model with a k parameter of ~0.6 agrees with observations the best, with model scatter comparable to that of Hapke model fitting for the inner part of the disk with i or e <50°, and smaller scatter (8%) than Hapke model fitting for outskirt. To explore potential better description of the limb profile for Ceres, we modified the Minnaert model to set free the power index of cos(e) term. The resulting model did the best job in describing the outskirt area of the disk (5% scatter) compared to the other two models, but not as well for center part, and disregarded. Both Hapke model and Minnaert model give similar results for photometric correction.

The small scatter in photometric modeling suggests that the albedo variation across the disk of Ceres is smaller than a few percent at the resolution of 60 km. The center part of the disk can be well mapped due the excellent job that photometric models do in describing the limb profile. But the areas with latitude >50° cannot be confidently mapped with these data due to the large scatters in photometric correction.

Constructing Global Maps: After photometric correction is applied to all images, they are projected into simple cylindrical frame of longitude and latitude and combined to make the global maps of Ceres.

An example is shown in Fig. 2. In order to combine all images and take the advantage of the shift between images on the disk of Ceres due to its rotation and pointing shift of HST to enhance the resolution of the maps, we projected all photometrically corrected images into an over-sampled cylindrical grid with a

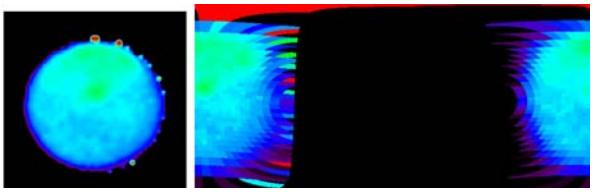

Fig. 2. Left panel shows a photometrically corrected image. Right panel is the projection of the left panel onto a cylindrical frame.

step size of 0.5° in both axes. Then for each grid point, its corresponding pixel position in the original images is calculated from the shape model of Ceres and the observing geometry. Because the resolution of images is much lower than 0.5°, each pixel in one image is projected to many grid points in the map, with different shapes in the projection (Fig. 2). Once all images are projected to make partial maps, these maps can be combined to complete the global maps.

To combine all partial maps, for each grid point in the map, we can simply take the average, or median, of the grid values of all partial maps that cover that grid point. For our case, since no cosmic ray rejection has been done by the standard HST data reduction pipeline due to the rotation of Ceres, median will be a better choice over average. For each grid point that is lower than latitude 40°, there are more than seven partial maps covering it. Thus in the combination of all partial maps, cosmic rays can be effectively rejected. The final map at 535 nm wavelength is shown in Fig. 3 as an example.

To assess the quality of the final maps, several test and evaluations are performed.

First, we need to make sure that the noise in the original images is at a low level to affect the mapping. The signal-to-noise ratio is estimated for all images, and found to be higher than 1000 for 535 nm images, 500 for 335 nm images, and 250 for 232 nm images.

Next step, we verified the projection from images to cylindrical frame is done correctly. By linking all photometrically corrected images (Fig. 2, left panel) in time sequence, the rotation of the disk can be easily seen by the movement of features crossing the disk. Similarly, by linking all partial maps (Fig. 2, right panel) projected from the photometric corrected images in time sequence, it is clearly seen that the covered area in the partial maps moves from east to west as Ceres rotations from west to east, while surface features just sit still in the their longitude and latitude position, with almost constant brightness. This demonstrates that features are consistently seen in multi images and are real, and they have been correctly projected onto the cylindrical frame of Ceres.

Finally, standard deviation maps are generated to assess how well the combination of partial maps has been done. We simply calculated the standard deviation for each grid position from the same grid positions in al partial maps that cover the particular grid, and then weighed by the cosine of emission angle to take into account the projection. For most grid positions, they are covered by more than 14 partial maps, therefore the standard deviation is a good assessment of error. If, however, for some grid positions there are only a few partial maps covering it, then the standard deviation is probably an underestimate of the error of that point. This could happen for areas close to the north and south edge of the final maps. But overall, the standard deviation is typically 1% for 535 nm map, and 10% for 223 nm map.

Discussions: The original HST observation was designed to take three images of one filter consecutively as a group before switch to the next in order to facilitate dithering to enhance the spatial resolution. The dithered images are released on HST website (http://hubblesite.org/newscenter/archive/releases/2005/27/) showing a great enhancement of resolution. We did not use dither in constructing our maps. In stead,

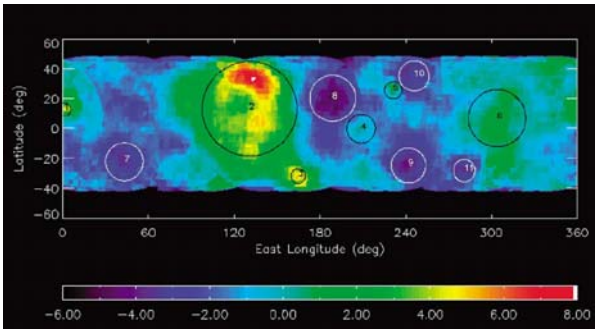

Fig. 3. Final map of Ceres at 535 nm wavelength. For maps at other two wavelengths, refer to [2].

we consider that the technique we used to combine images has the effect of dithering but with limitations.

The cylindrical frame we projected all images onto is highly super-sampled. We calculated for the grids of the cylindrical frame their pixel positions in the original images. The calculation was essentially done in a sub-pixel sense. Thus slight pointing shift between images will result in slightly different projected position in the super-sampled cylindrical frame. Combining all partial maps, we effectively took the advantage of the sub-pixel pointing shift between images to enhance the resolution. However, the caveat is that no point spread function (PSF) has been taken into account. For any pixel, its intensity is affected by pixels surrounding it depending on the shape of PSF. This is what has been taken care of by the well developed dithering algorithm.

Reference: [1] Thomas, P. C. *et al.*, (2005) *Nature*, *437*, 224-226; [2] Li, J.-Y. *et al.* (2006) *Icarus*, *182*, 143-160.